

# Cell Wall Hydrolases Affect Germination, Vegetative Growth, and Sporulation in *Streptomyces coelicolor*<sup>▽†</sup>

Henry J. Haiser, Mary R. Yousef, and Marie A. Elliot\*

Department of Biology and Michael G. DeGroote Institute for Infectious Disease Research, McMaster University,  
1280 Main Street West, Hamilton, Ontario L8S 4K1, Canada

Received 12 June 2009/Accepted 20 August 2009

**Peptidoglycan is a major cell wall constituent of gram-positive bacteria. It is a dynamic macromolecule that is actively remodeled to enable cell growth and differentiation through a tightly choreographed interplay of hydrolytic and biosynthetic enzyme activities. The filamentous bacterium *Streptomyces coelicolor* has a complex life cycle that likely requires considerable cell wall remodeling to enable both extension of vegetative hyphae and formation of differentiated cell types. In silico analysis of the *S. coelicolor* genome enabled identification of 56 candidate cell wall hydrolase genes. We found that seven of these genes shared a highly conserved 5' untranslated region and were expressed during both vegetative growth and sporulation; four of these genes were selected for more extensive biochemical and biological characterization. The proteins encoded by these genes, termed RpfA, SwlA, SwlB, and SwlC, were confirmed to be hydrolytic enzymes, as they could efficiently cleave *S. coelicolor* cell walls. Phenotypic analyses revealed that these enzymes are important throughout development; deletion of each hydrolase gene resulted in a mutant strain that was heat sensitive, defective in spore formation, and either altered in vegetative growth or delayed in spore germination. Our results indicate that these enzymes play key roles at multiple stages in the growth and development of *S. coelicolor*, highlighting both the lack of redundancy in hydrolase activity and the importance of cell wall remodeling in the *S. coelicolor* life cycle.**

Peptidoglycan (PG) is a primary constituent of the gram-positive bacterial cell wall and, despite its rigid structure, is a remarkably dynamic macromolecule. It functions in maintaining cell shape and cytoplasmic turgor pressure and serves as the scaffolding to which cell wall-associated components, such as proteins and teichoic acids, are anchored (16). PG comprises alternating *N*-acetylglucosamine and *N*-acetylmuramic acid residues, which make up the glycan backbone, and peptide side chains that link the glycan strands together (49). PG biosynthesis is a complex process involving the concerted efforts of many enzymes, beginning with precursor synthesis in the cytoplasm and concluding with polymerization outside the cytoplasmic membrane (3, 8, 48). During bacterial growth, PG is actively remodeled to allow incorporation of new PG and to accommodate changes in cell shape. The enzymes responsible for this remodeling are collectively termed cell wall hydrolases, and they act by cleaving covalent bonds within either the glycan strands or the peptide side chains. The essential nature of PG requires that synthesis and cleavage be tightly regulated, with the activities of biosynthetic and hydrolytic enzymes coordinated in both space and time.

Cell wall hydrolases are diverse enzymes that are typically grouped on the basis of substrate specificity and the resulting cleavage products. The major groups include the lysozymes and lytic transglycosylases, which hydrolyze the  $\beta$ -(1,4)-glyco-

sidic linkage between *N*-acetylmuramic acid and *N*-acetylglucosamine; the endopeptidases, which cleave the peptide bonds in the amino acid side chains connecting the parallel glycan strands; the carboxypeptidases, which cleave the C-terminal amino acids of peptide chains; and the amidases, which cleave between *N*-acetylmuramic acid and the first residue (L-Ala) of the peptide side chain (55).

In addition to remodeling the PG, cell wall hydrolases also contribute to a multitude of specialized cellular processes, from the assembly of secretion systems, flagella, and pili (55) to the resuscitation of dormant cells by a recently discovered class of hydrolases known as the resuscitation-promoting factors (Rpf) (37). The Rpf are secreted proteins that are structurally related to lysozymes (12, 13) and are found in a subset of the actinomycetes, including *Micrococcus*, *Mycobacterium*, *Corynebacterium*, and *Streptomyces* (44). The sole *Micrococcus luteus* Rpf is essential for viability (36), while in *Mycobacterium tuberculosis*, which encodes five Rpf proteins, the enzymes are required for virulence and resumption of active growth during emergence from a latent state (26). The sporulating actinomycete *Streptomyces coelicolor* is predicted to encode seven Rpf proteins, along with a plethora of other cell wall hydrolases. Surprisingly little is known about cell wall remodeling in the streptomycetes, despite the fact that significant remodeling must accompany the filamentous growth and morphological changes associated with the different stages of the *Streptomyces* life cycle. The *S. coelicolor* life cycle initiates with spore germination; this process likely depends on cell wall hydrolase activity, as spore germination in *Bacillus subtilis* requires the activity of at least two hydrolases (50). Following spore germination in *S. coelicolor*, germ tubes elongate and branch in a filamentous manner, forming a network of cells termed the

\* Corresponding author. Mailing address: Department of Biology, McMaster University, 1280 Main Street West, Hamilton, ON L8S 4K1, Canada. Phone: (905) 525-9140, ext. 24225. Fax: (905) 522-6066. E-mail: melliot@mcmaster.ca.

† Supplemental material for this article may be found at <http://jb.asm.org/>.

<sup>▽</sup> Published ahead of print on 28 August 2009.

TABLE 1. Predicted cell wall hydrolases encoded in the *S. coelicolor* genome

Hydrolase group or subgroup	Function	Genes	Reference(s)
<i>N</i> -Acetylmuramidase/ <i>N</i> -acetylglucosaminidase (including lysozyme, lytic transglycosylase, Slt, and GEWL-like domains)	Cleaves between MurNAc and GlcNAc (muramidase) and GlcNAc and MurNAc (glucosaminidase)	SCO0543, SCO0591, SCO1805, SCO2001, SCO2409, SCO4132, SCO4582, SCO4820, SCO5029, SCO5286, SCO5466, SCO5997	54
Resuscitation-promoting factor (Rpf) subgroup	Cleaves between MurNAc and GlcNAc	SCO0974, SCO2326, SCO3097, <sup>a</sup> SCO3098, <sup>a</sup> SCO3150, SCO5029, SCO7458	44
Carboxypeptidase	Removes C-terminal L or D amino acid	SCO0088, SCO3408, SCO3774, SCO3811, SCO4439, SCO4847, SCO5467, SCO5660, SCO6131, SCO6489, SCO7050, SCO7607	
Endopeptidase	Cleaves amide bonds in peptides	SCO2835, SCO3368, SCO3949, SCO4082, SCO4132, SCO4561, SCO4672, SCO4798, SCO5623, SCO5839, SCO6773 <sup>a</sup>	
NlpC/P60 subgroup	Endopeptidase/amidase activity	SCO1240, SCO2135, SCO2136, SCO3511, SCO4108, SCO4202, SCO4793, SCO4796, SCO5294, SCO6884, SCO7021, SCP1148	2
Amidase	Cleaves between lactyl group of MurNAc and L-Ala	SCO1172, SCO2116, SCO2313, SCO5487, SCO7179, SCO7250	

<sup>a</sup> Gene encoding protein containing a LysM PG-binding domain.

vegetative mycelium. A second type of filamentous (but non-branching) cells, the aerial hyphae, then emerge from the vegetative mycelium, and it is within these cells that chains of spores develop. Cell wall hydrolase activity and the associated cell wall remodeling are thought to be essential for vegetative hyphal branch formation, vegetative and aerial hyphal tip extension, spore chain formation, and spore dispersal. In this work, we describe the first investigation of cell wall hydrolase activity and function in *Streptomyces*. We identify a subset of hydrolases whose genes share a conserved 5' untranslated region (UTR), demonstrate enzymatic activity for four of these proteins, and reveal that these enzymes function at multiple stages in the *S. coelicolor* life cycle.

#### MATERIALS AND METHODS

**Bioinformatic search for cell wall hydrolase enzymes.** Amino acid sequences corresponding to characterized cell wall hydrolases from both gram-positive and gram-negative bacteria and representing each of the functional categories listed in Table 1 were used to identify candidate cell wall hydrolases in *S. coelicolor*. The following query sequences were obtained from the ExPASy database (<http://ca.expasy.org/sprot/>): Slt70 from *Escherichia coli* (18) and the conserved Rpf domain (44) for the *N*-acetylglucosaminidases; DacB from *E. coli* (29) for the carboxypeptidases; LytE from *Bacillus subtilis* (33) and multiple protein sequences housing the NlpC/P60-like domain as described by Anantharaman and Aravind (2) for the endopeptidases; and CwlA from *B. subtilis* (30) for the amidases. The sequences were subjected to BLASTp analysis (1) against the sequenced genome of *S. coelicolor* A3(2) (7). The *Streptomyces* annotation server (<http://streptomyces.org.uk/>) was also used to identify cell wall hydrolase candidates, which were further validated by the conserved domain function of BLASTp. Potential candidates with an E value of  $<10^{-4}$  and possessing  $>25\%$  identity over 100 amino acids were included. Signal peptides were predicted using SignalP 3.0 (6).

**Bacterial strains and culture conditions.** *S. coelicolor* A3(2) wild-type strain M145 and mutant derivatives (Table 2) were grown on R2YE or R5 (rich) and MS (mannitol-soy flour) agar media or in liquid tryptic soy broth supplemented with antibiotics to maintain selection when appropriate. The growth medium composition and standard culture techniques used have been described previously (28). *E. coli* strains used for cloning and protein overexpression are indicated in Table 2. Standard *E. coli* growth conditions for DNA manipulation and protein purification were used (47).

**RNA isolation.** Cultures were grown on agar plates overlaid with cellophane disks, and once desired stages of growth were reached, mycelia were scraped off and total RNA was harvested as described previously (21). All RNA samples were quantified by UV spectroscopy using an Ultrospec 3100 pro (Biochrom), and RNA quality was assessed by agarose gel electrophoresis.

**Transcript end mapping.** S1 nuclease mapping was performed as described previously (17). Reaction products were separated on 6% denaturing polyacrylamide sequencing gels. Sizes were estimated by running an end-labeled 100-bp ladder beside samples. 5' rapid amplification of cDNA ends (RACE) was carried out using an RNA ligase-mediated (RLM) RACE kit (Applied Biosystems) according to the manufacturer's instructions with minor modifications, as described previously (53).

**RT-PCR.** Total RNA samples were subjected to reverse transcription (RT) using SuperScript III reverse transcriptase (Invitrogen). The annealing reaction mixtures consisted of 2 pmol of gene-specific primer (see Table S1 in the supplemental material), 1  $\mu$ g total RNA, and 2  $\mu$ l of a 5 mM deoxynucleoside triphosphate mixture. The annealing reaction mixture was incubated at 65°C for 5 min, followed by 1 min of incubation on ice and subsequent addition of 4  $\mu$ l 5 $\times$  First-Strand buffer, 1  $\mu$ l 0.1 M dithiothreitol, 40 U RNaseOUT (Invitrogen), and 200 U SuperScript. The RT reaction mixture and subsequent addition were mixed and then incubated at 55°C for 1 h, which was followed by 15 min of incubation at 70°C to inactivate the enzyme. Following RT, PCR mixtures were prepared using 2  $\mu$ l cDNA, 0.5  $\mu$ l each 50  $\mu$ M gene-specific primer (see Table S1 in the supplemental material), 1  $\mu$ l 5 mM deoxynucleoside triphosphate mixture, 2.5  $\mu$ l 10 $\times$  PCR buffer, 2.5  $\mu$ l 20 mM MgSO<sub>4</sub>, 2.5  $\mu$ l 50% dimethyl sulfoxide, 1.25 U Taq DNA polymerase (UBI), and enough distilled H<sub>2</sub>O (dH<sub>2</sub>O) to obtain a final volume of 25  $\mu$ l. The PCR mixtures were heated at 95°C for 5 min; optimal annealing temperatures were determined empirically and varied between 58 and 64°C for 45 s; the extension time was 45 s for all reactions; and the number of cycles varied between 15 and 28 cycles for the template-primer pairs to ensure that products were generated during the exponential phase of the reaction (within the linear range of amplification). Ten microliters of each PCR mixture was separated on 2% agarose gels and visualized by ethidium bromide staining. The controls for RT-PCR included 16S rRNA as a positive control for RNA integrity and equal RNA loading and a "no-RT" sample as a negative control for each template-primer combination to ensure that reaction mixtures were not contaminated with DNA.

**Protein overexpression and purification.** DNA fragments encompassing the predicted binding and catalytic domains of each protein of interest were PCR amplified using the iProof polymerase system (Bio-Rad) by following the manufacturer's recommendations (see Table S1 in the supplemental material for oligonucleotide sequences). In each case, the region encompassing the SignalP-predicted signal peptide was not included in the DNA to be cloned. PCR products were purified using a PCR purification kit (Qiagen). Purified DNA

TABLE 2. Bacterial strains and plasmids used in this study

Strain	Genotype, characteristics, and/or use	Reference or source
<i>Streptomyces coelicolor</i> A3(2) strains		
M145	SCP1 <sup>−</sup> SCP2 <sup>−</sup>	28
E103 ( <i>swlA</i> )	M145 SCO1240:: <i>aac(3)IV</i>	This study
E104 ( <i>rpfA</i> )	M145 SCO3097:: <i>aac(3)IV</i>	This study
E105 ( <i>swlB</i> )	M145 SCO4582:: <i>aac(3)IV</i>	This study
E106 ( <i>swlC</i> )	M145 SCO6773:: <i>aac(3)IV</i>	This study
E107 ( <i>rpfA swlB</i> )	M145 SCO3097:: <i>vph</i> SCO4582:: <i>aac(3)IV</i>	This study
E108 ( <i>rpfA swlB swlC</i> )	M145 SCO3097 SCO4582:: <i>aac(3)IV</i> SCO6773:: <i>vph</i>	This study
<i>Escherichia coli</i> strains		
DH5 $\alpha$	Used for routine cloning	
ET12567(pUZ8002)	<i>dam dcm</i> ; with <i>trans</i> -mobilizing plasmid pUZ8002	32, 42
BL21(DE3)(pLysS)	Protein overexpression host	Novagen
Rosetta 2	Protein overexpression host with pRARE2, which supplies “rare” tRNAs	Novagen
Plasmids		
BT340	FLP recombination plasmid	14
pIJ82	pSET152 derivative, <i>aac(3)IV</i> replaced with <i>hyg</i> gene	Gift from H. Kieser
pIJ2925	pUC18-based cloning vector	25
pET15b	Overexpression of His <sub>6</sub> -tagged proteins	Novagen

fragments were sequentially digested with the BamHI and NdeI restriction endonucleases. The resulting fragments were ligated into the expression vector pET15b (Novagen), which had been similarly digested with BamHI and NdeI, before they were dephosphorylated. Inserts were confirmed by sequencing with T7 promoter and terminator primers (see Table S1 in the supplemental material). Constructs were then transformed into either *E. coli* Rosetta2 or *E. coli* BL21(DE3)/pLysS (Novagen). Overexpression trials with small-volume cultures were carried out by subculturing the plasmid-containing strains to the exponential growth phase, inducing them with isopropyl- $\beta$ -D-thiogalactopyranoside (IPTG), and monitoring the growth for various periods of time and at different temperatures to empirically determine the best conditions for overexpression of soluble protein (see Table S2 in the supplemental material for optimal conditions). Proteins were then purified by incubating lysates from overexpressing cells with Ni-nitrilotriacetic acid agarose resin (Qiagen) and passing the resulting slurry through PolyPrep chromatography columns (Bio-Rad). Three washes were performed using increasing concentrations of imidazole (20 mM to 200 mM), before purified protein was eluted with either 250 mM (RpfA and SwlB) or 500 mM (SwlA and SwlC) imidazole. Pure protein was examined by separating aliquots of each eluate on 12% or 15% sodium dodecyl sulfate (SDS)-polyacrylamide gels, and each protein was estimated to be ~90% pure by subsequent staining with Coomassie blue. Proteins were quantified by the Bradford assay (9), using bovine serum albumin and lysozyme as standards.

***S. coelicolor* cell wall harvest.** Cultures were grown in liquid tryptic soy broth for ~48 h, after which cells were collected by centrifugation. The cell pellet was resuspended in a 1% SDS solution and boiled for 30 min, followed by centrifugation at 13,793  $\times g$  for 30 min. This procedure was repeated once before a series of washes in 60°C dH<sub>2</sub>O were carried out. After the final wash in dH<sub>2</sub>O, the pellet was resuspended in acetone, and the cell wall preparation was spun down one final time before it was air dried. The dry weight of the cell wall preparation was then determined. Cell wall material was then used in zymogram assays (see below).

**Cell wall hydrolase activity assay.** Zymograms were used to assay the putative cell wall hydrolases for cleavage activity (31). Cell wall material was incorporated into SDS-polyacrylamide (0.1%, wt/vol) gels, with which purified proteins were separated. Following electrophoresis, gels were incubated in renaturation buffer (see Table S2 in the supplemental material) overnight at 30°C. Gels containing renatured proteins were then stained with 0.1% methylene blue, 0.01% KOH for 2 h, which was followed by several washes with dH<sub>2</sub>O to destain them. Zones of clearing indicated cell wall hydrolysis by the purified proteins. The controls for the zymogram analysis included purified lysozyme (BioShop) as a positive control and a purified His<sub>6</sub>-tagged transcription factor (Crp) from *S. coelicolor* (not expected to possess cell wall cleavage activity) as a negative control. Zymograms were run in parallel with Coomassie blue-stained gels to confirm that the proteins migrated at the expected sizes compared to the size markers.

**Hydrolase mutant strain construction.** Single null mutations of the coding regions for the cell wall hydrolases were created using a standard PCR-targeted

gene replacement technique (20). The *aac(3)IV* (apramycin) resistance cassette from pIJ773 (20) was used to create all single mutations. An *rpfA swlB* double-mutant strain was created by replacing the *swlB* gene in the *rpfA::aac(3)IV* strain with a *vph* (viomycin) resistance cassette from pIJ780 (20). An *rpfA swlB swlC* triple-mutant strain was constructed by first removing the viomycin cassette that had replaced *swlB* in the *rpfA swlB* double-mutant strain via FLP recombinase-mediated excision as described previously (17, 20) and then replacing the *swlC* coding region with the viomycin resistance cassette. Mutant cosmids used in the disruption procedure were confirmed by digestion and PCRs performed with several combinations of primers upstream of, inside, and downstream of the disrupted gene. *S. coelicolor* mutant strains were confirmed by PCRs like the cosmid mutants (data not shown).

**Construction of complementation vectors.** Mutant strains were complemented by cloning DNA corresponding to the coding region (in the case of *rpfA*, this included SCO3098), along with extended upstream and downstream sequences in order to include all regulatory elements, into the integrating *Streptomyces* vector pIJ82 (Table 3; see Table S1 in the supplemental material). Constructs were introduced into mutant strains via conjugation between the complementation plasmid-containing *E. coli* strain ET12567/pUZ8002 (which mobilizes the *oriT*-containing plasmid pIJ82 for conjugation in *trans*) (Table 2) and the corresponding *S. coelicolor* mutant. Empty plasmid controls were also introduced into the mutant strains. Complementation was assessed by comparing the phenotypes of the wild-type strain, the mutant, the mutant containing an empty plasmid, and the mutant containing the complementing plasmid under appropriate growth or stress conditions.

**SEM and TEM.** Mutant and wild-type strains were streaked to obtain single colonies on MS agar and grown for 4 to 5 days. Individual colonies were excised

TABLE 3. 5' end mapping of the seven cell wall hydrolase transcripts

Gene	Predicted protein function or domain	Predicted leader size (nt) <sup>a</sup>	UTR size based on S1 mapping (nt)	UTR size based on 5' RACE (nt)
SCO1240 ( <i>swlA</i> )	NlpC/P60	183	~100	
SCO3097 ( <i>rpfA</i> )	Rpf	166	~240	237
SCO4108	Endopeptidase	155		207
SCO4582 ( <i>swlB</i> )	Transglycosylase	123		162
SCO4796	NlpC/P60	182	~180	
SCO5839	Endopeptidase	160	~200	
SCO6773 ( <i>swlC</i> )	Endopeptidase	155		205

<sup>a</sup> Data from reference 4.



from a plate and prepared for scanning electron microscopy (SEM) or transmission electron microscopy (TEM). Samples were fixed overnight in 2% glutaraldehyde, rinsed twice in dH<sub>2</sub>O, and postfixed in 1% osmium tetroxide for 1 h. Samples were then dehydrated using an ethanol gradient (50%, 70%, 95%, and 100% ethanol). SEM samples were transferred to a critical point dryer and, once dry, were mounted onto SEM stubs and coated with gold before they were viewed using a JEOL JSM 840 SEM. TEM samples were subjected to a final dehydration in 100% propylene oxide, infiltrated with Spurr's resin, and transferred to an embedding mold, where they were polymerized in Spurr's resin at 60°C overnight. Sections were then cut using a Leica UCT ultramicrotome and viewed using a JEOL JEM 1200 TEM. All images were analyzed using ImageJ 1.41a and Adobe Photoshop CS version 8.0 software. The spore diameter and spore wall thickness were calculated for at least 25 spores for each strain.

**Light microscopy and DAPI staining.** Samples for light and fluorescence microscopy were obtained by taking coverslip impressions of samples incubated for 4 days on MS agar. Samples were stained with 4',6-diamidino-2-phenylindole (DAPI). All images were obtained using a Leica wide-field fluorescence microscopy system with a Leica HCS Plan Apo oil immersion objective (magnification,  $\times 100$ ; numerical aperture, 1.4; Leica Microsystems, Wetzlar, Germany). Digital images were processed using Adobe Photoshop CS version 8.0 software.

**Heat shock assay.** Spore suspensions of wild-type and mutant strains were diluted with dH<sub>2</sub>O to obtain a final concentration of  $\sim 300$  spores/50  $\mu$ l and placed in a 60°C water bath. Fifty-microliter aliquots were plated on MS agar after the incubation times indicated below, and the plates were then incubated at 30°C for  $\sim 5$  days. Survival rates were calculated by dividing the number of colonies on plates after heat treatment by the number of colonies on plates without heat treatment and were expressed as percentages.

**Lysozyme and cell wall antibiotic sensitivity assays.** Sensitivities to lysozyme, SDS detergent, and cell wall antibiotics were examined by placing paper disks containing a test compound onto minimal medium agar plates (28) freshly spread with spores to obtain a confluent lawn. After 3 days of incubation at 30°C, zones of growth inhibition were measured for all strains, and the inhibition zones for the mutant strains were compared to those for the wild type. Lysozyme (BioShop) was tested using 3, 0.3, and 0.03 mg/ml lysozyme; SDS sensitivity was examined using 10%, 1%, and 0.1% SDS; and the antibiotics phosphomycin, vancomycin, cefuroxime, bacitracin, nafcillin, and D-cycloserine were tested by applying 320  $\mu$ g of each antibiotic to the disks.

**Germination assay.** To assess the timing of germination in mutant and wild-type strains, spores were plated on MS agar overlaid with cellophane disks and incubated at 30°C. At specific time points (3 h, 5.5 h, 6.5 h, 7.5 h, 9 h, and 11 h), a portion of a cellophane disk (1 cm by 1 cm) was excised and viewed with a light microscope to score germinated spores (indicated by the presence of one or more germ tubes) and nongerminated spores. The data are representative of at least two independent experiments, and a minimum of 200 spores were counted in each experiment.

## RESULTS

**In silico identification and analysis of cell wall hydrolases in *S. coelicolor*.** We anticipated that cell wall remodeling was critical for the growth and morphological development of *S. coelicolor*. Given this, we conducted a survey of the *S. coelicolor* A3(2) genome to identify potential cell wall hydrolase candidates. Using BLASTp analyses and experimentally validated bacterial hydrolases as our query sequences, we identified 60 potential hydrolases in *S. coelicolor* having  $>25\%$  sequence identity to known hydrolase domains over the majority of the domain sequence. To put this into context relative to other bacteria, *B. subtilis*, another gram-positive, soil-dwelling, spore-forming bacterium, is predicted to encode 35 cell wall hydrolases (51), while *Lactococcus lactis* is predicted to encode 10 cell wall hydrolases (52) and the gram-negative organism *E. coli* is predicted to encode 30 cell wall hydrolases (24). *S. coelicolor*, therefore, encodes a significantly greater number of cell wall hydrolases than other bacteria, and this likely reflects the complexity of the *Streptomyces* life cycle. We have assigned the 60 *S. coelicolor* hydrolases to four functional groups: *N*-acetylglucosaminidases, carboxypeptidases, endopeptidases,

and amidases (Table 1). The group containing the most enzymes was the endopeptidase group, with 23 enzymes. Of these, 12 were identified as NlpC/P60-like proteins. The majority of functionally characterized NlpC/P60 enzymes possess endopeptidase activity (2), but there are also examples of enzymes with amidase activity (19) and for this reason these proteins have been assigned to a distinct subgroup (Table 1). The *N*-acetylglucosaminidases/muraminidases are also well represented, and 19 predicted enzymes belong to this group. Seven of these enzymes have previously been designated members of the Rpf subgroup, although in this group the SCO2326 and SCO5029 proteins are predicted to have domains only distantly related to the Rpf domain (44). Interestingly, only 3 of the 60 hydrolases identified in our screen are predicted to possess LysM domains (SCO3097, SCO3098, and SCO6773) (Table 1). These domains are involved in PG binding and are commonly associated with cell wall hydrolases (10).

While none of the predicted hydrolases have been characterized, members of the Rpf class have been studied extensively in other actinomycetes (38, 39). Analysis of the *rpf* genes in *S. coelicolor* revealed that the sequence upstream of one gene, SCO3097 (also referred to as *rpfA*), is highly conserved in the upstream regions of six other cell wall hydrolase genes: SCO1240, SCO4108, SCO4582, SCO4796, SCO5839, and SCO6773 (Fig. 1A). The associated products of these seven genes are predicted to have diverse enzymatic activities (5). *rpfA* encodes one of the Rpf-like enzymes with a LysM PG-binding motif; SCO1240 and SCO4796 encode putative NlpC/P60 endopeptidases/amidases; SCO4582 is predicted to encode an enzyme with lytic transglycosylase activity; and SCO4108, SCO5839 and SCO6773 are predicted to encode endopeptidases (the SCO6773 product also contains a LysM domain) (Fig. 1B). We renamed SCO1240 (*swlA*), SCO4582 (*swlB*), and SCO6773 (*swlC*) for reasons that are described below. The upstream sequence conservation for these seven genes was found to be maintained for orthologous genes in multiple *Streptomyces* species, including *Streptomyces avermitilis* and *Streptomyces griseus* (see Fig. S1 in the supplemental material), as well as in more divergent gram-positive bacteria (4). Barrick et al. (4) identified the upstream sequence as a potential riboswitch. Riboswitches are RNA sequences typically found within the leader UTRs of mRNAs and range in size from 40 to 150 nucleotides (nt) (46, 56). They adopt structures that bind metabolites with exquisite specificity, and this binding often results in a structural alteration that modulates either the transcription or translation of the associated downstream gene(s). The products of genes downstream of similar riboswitches usually act in common pathways, and given this, we set out to elucidate the biological roles of these hydrolase genes and their associated products, guided by the expectation that they may act together to facilitate a specific aspect of cell wall remodeling in *Streptomyces*.

**Seven cell wall hydrolase genes have distinct transcription profiles.** As a first step in characterizing the seven genes, we sought to determine whether they were subject to common transcriptional or posttranscriptional control. To investigate their expression profiles, RNA was harvested from plate-grown cultures at growth stages ranging from early vegetative growth to sporulation. Following harvesting of RNA, semiquantitative RT-PCR was conducted (as hydrolase genes are often ex-

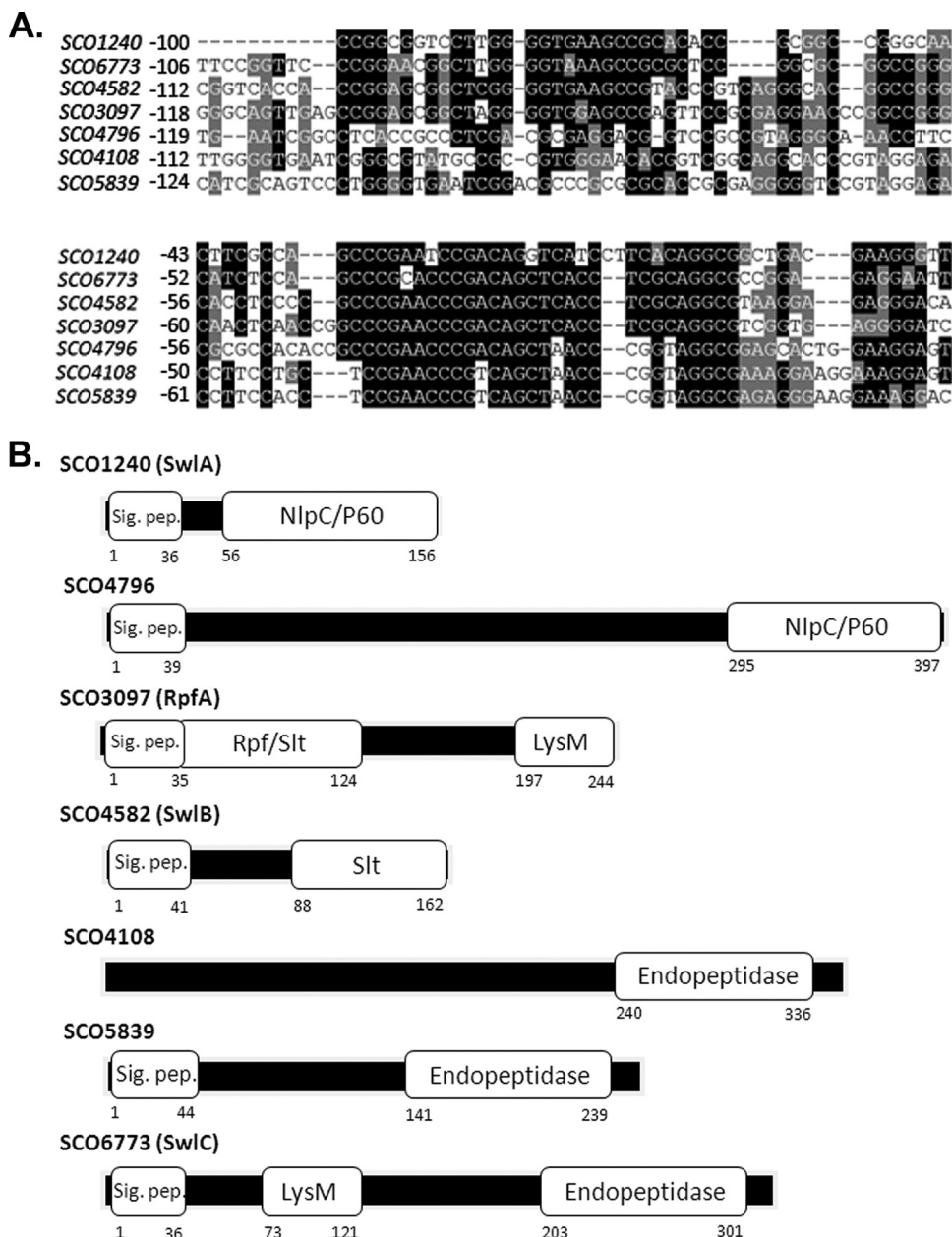


FIG. 1. Analysis of coding and noncoding sequences for seven putative cell wall hydrolases sharing a conserved upstream sequence. (A) Multiple-sequence alignment of the predicted UTRs (4) of the seven hydrolase-encoding genes. Identical nucleotides are indicated by a black background, while similar nucleotides (purines or pyrimidines) are indicated by a gray background. (B) Schematic representation of the functional domains identified in the seven cell wall hydrolase proteins. Proteins are grouped on the basis of the functional domain, with the relative position of each domain within the protein sequence indicated by the amino acid number at the beginning and end of each domain or motif. Abbreviations: Sig. pep., signal peptide; NlpC/P60, endopeptidase domain; Slt, soluble lytic transglycosylase; Rpf, resuscitation-promoting factor; LysM, lysin motif (implicated in peptidoglycan binding).

pressed at low levels), and various transcriptional patterns were observed. The expression of four of the genes (*rpfA*, SCO4582, SCO5839, and SCO6773) peaked at 24 h, after which their expression appeared to decline before it increased again during sporulation (48 h) (Fig. 2). A similar profile was observed for SCO4108 and SCO4796, except that for these two genes the maximal transcript levels were maintained for an extended period (24 to 31 h) before the levels decreased and then increased again during entry into the sporulation stage. In

contrast, SCO1240 expression increased throughout development, and maximal transcript abundance occurred at 48 h (during spore formation). These expression profiles were reproducibly observed with both experimental and biological replicates. The variable expression patterns observed for the seven genes suggested that they were unlikely to be coordinately regulated at a transcriptional or posttranscriptional (transcript stability) level, although such regulation may be shared by subsets of these seven genes.

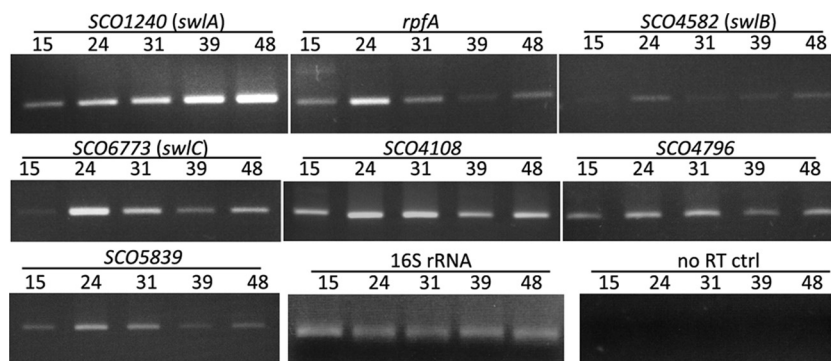


FIG. 2. Expression profiles of the putative cell wall hydrolase genes during *S. coelicolor* development. RNA was harvested after 15, 24, 31, 39, and 48 h of growth on R5 (rich) medium. Vegetative hyphae were evident at 15 h, aerial hyphae were beginning to form by 24 h, and spores were detectable by 48 h. RNA samples were subjected to RT-PCR using oligonucleotides specific for the coding regions of the seven hydrolase genes. The number of reaction cycles was optimized for each PCR to ensure that the products examined were generated within the linear range of amplification (27 cycles for SCO1240, SCO4108, SCO4796, and SCO5839; 28 cycles for *rpfA*, SCO4582, and SCO6773). 16S cDNA was amplified as a positive control (15 cycles), and a “no-RT” reaction was conducted using each template-primer combination to ensure there was no DNA contamination of the RNA samples or the PCR reagents (27 or 28 cycles).

**The conserved upstream sequence corresponds to an extended 5' UTR.** Given the different transcription profiles observed for the hydrolase-encoding genes, we decided to test whether the conserved upstream sequence did in fact correspond to a leader UTR, as the “riboswitch” designation was based solely on bioinformatic analyses and there is no experimental data to support its existence. We first investigated whether this sequence could be part of the coding sequence for each gene due to misannotation of translation start sites. We found that each annotated translation start site was preceded by a strong ribosome-binding site and that six of the seven genes either had no alternative start codons within 300 nt of the annotated start or had a stop codon located between any potential start codon and the annotated start (*rpfA* had an alternative start codon 15 nt upstream of the predicted start site). This suggested that translation was unlikely to initiate within the conserved upstream sequence.

Using S1 nuclease mapping and 5' RACE experiments, we mapped the transcription start sites for each gene and found that each message included an extended 5' UTR (Table 3). The SCO1240 transcript had the shortest 5' UTR (~100 nt), while the other transcripts had longer leaders, which ranged from 162 nt long for SCO4582 to 237 nt long for *rpfA*. The mapped end was ~40 to 50 nt longer than the size of the leader predicted by the previous bioinformatic analyses (4) for all seven hydrolase genes except SCO4796, whose leader sequence was the predicted size, and SCO1240, whose leader sequence was ~80 nt shorter than the expected size.

**Purified cell wall hydrolases cleave *S. coelicolor* cell walls.** Having established that each of the hydrolase genes shared a conserved leader region large enough to include a riboswitch and taking into account that common riboswitches are associated with common pathways, we turned our attention to the function of the associated gene products, investigating whether these proteins were required at specific times during *Streptomyces* development. The seven enzymes fell into four distinct functional classes, and in order to focus our investigations, we decided to select one enzyme from each functional class for further biochemical and biological characterization, as follows:

RpfA (LysM-containing Rpf subclass), SCO1240 (NlpC/P60 endopeptidase/amidase), SCO4582 (lytic transglycosylase), and SCO6773 (LysM-containing endopeptidase). To probe the enzymatic functions of these enzymes, they were overexpressed as N-terminal His-tagged fusions (without their signal peptides) and were purified using Ni<sup>2+</sup> affinity chromatography. Each enzyme was assessed for its ability to cleave purified cell wall preparations from wild-type *S. coelicolor* using zymogram analysis, a standard method for demonstrating cell wall hydrolase activity (31). All four hydrolases had detectable cleavage activity, as evidenced by zones of clearing on the zymogram (Fig. 3), although not all of them were equally effective in their cleavage capabilities. SCO6773 (SwlC) exhibited the most robust cleavage of the four enzymes and was also the most stable, retaining its activity for several weeks, in contrast to the other enzymes, all of which lost cleavage activity within days. SCO4582 (SwlB) was readily purified; however, it exhibited less activity than equivalent amounts of SCO6773 (SwlC), and obtaining detectable cleavage in the zymogram assays required considerable buffer optimization (see Table S2 in the supplemental material). SCO1240 (SwlA) and RpfA were the least active of the four hydrolytic enzymes; they were the most challenging to overexpress and purify in an active form and were the least stable of the four enzymes examined in terms of their activity, although detectable zones of cleavage could be observed in the zymograms when freshly purified protein was used (Fig. 3). These experiments demonstrated cell wall cleavage capabilities for all four hydrolytic enzymes, and consequently, we propose that SCO1240, SCO4582 and SCO6773 be renamed SwlA, SwlB, and SwlC, respectively (*Streptomyces* cell wall lytic enzyme).

**SwlB and SwlC are important for branching during vegetative growth.** To shed light on the biological role of each of the four representative hydrolases and to determine whether these enzymes acted at similar stages in development, deletion mutants with individual mutations and combinations of mutations were constructed. As we had shown that the hydrolases could metabolize cell walls and given that the transcription of three of the four hydrolases (*rpfA*, *swlB*, and *swlC*) was maximal at



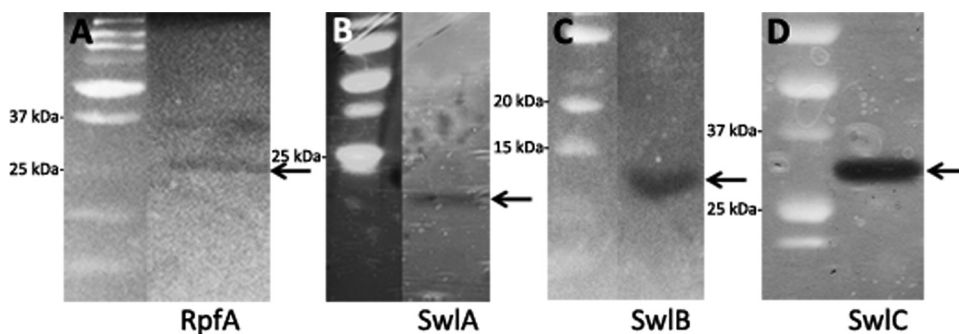


FIG. 3. Cell wall cleavage assay (zymogram) using *S. coelicolor* cell walls as the substrate. Purified cell wall hydrolases (without their signal peptides) were separated on a 12% or 15% polyacrylamide gel containing 0.2% *S. coelicolor* cell wall as the substrate. Following electrophoresis, the separated proteins were renatured for 18 h before the gel was stained with methylene blue to reveal zones of clearing, which represented cleavage of the cell wall. Precision Plus protein standards (Bio-Rad) were used as size markers for comparison with the following expected protein sizes: RpfA, 21.7 kDa (A); SwlA, 13.8 kDa (B); SwlB, 14.0 kDa (C); and SwlC, 28.6 kDa (D). Zones of clearing (indicated by arrows) are black bands on the inverted greyscale images. The second, larger band in panel A was reproducibly detected, but the corresponding protein could not be detected on a Coomassie blue-stained gel.

24 h, we reasoned that the absence of these gene products may affect vegetative growth. In examining the vegetative growth of plate-grown cultures, we found that *rpfa* and *swlA* mutants resembled the wild-type strain in their hyphal extension and branching patterns; however, the *swlB* mutant was markedly different. The vegetative hyphae of the *swlB* mutant appeared to be unusually long and straight, and there was a general lack of productive branching, where it appeared that branches could initiate, but continued outgrowth of these hyphae did not occur as robustly as it did in the wild type (Fig. 4). A similar phenotype was observed for the *swlC* mutant (data not shown). Both the *swlB* and *swlC* mutants grew at rates similar to the wild-type rate, and while emergence of the first branch initiated at the same position as in the wild type (i.e., there was no significant difference in the distance from the tip to the first branch) (data not shown), the resulting branches were significantly shorter for both of these mutants than for the wild type ( $P < 0.01$ ) (Fig. 4). The vegetative defects of the two mutants could be complemented by introduction of a wild-type copy of the gene into the chromosome (Fig. 4; data not shown).

**All cell wall hydrolase mutants form defective dormant spores.** The expression of the four hydrolase genes was also observed to increase during entry into the sporulation stage. Thus, we predicted that the products of these genes may also play a role in spore formation. Dormant *Streptomyces* spores are typically resistant to heat, and heat sensitivity is a hallmark of spore wall defects (33, 34). We therefore conducted heat shock assays with hydrolase mutants having individual mutations and with hydrolase mutants having combinations of mutations. All four single mutants were hypersensitive to heat stress; 10 min of exposure to 60°C resulted in ~70% viable wild-type spores, compared with ~30% viable spores for the mutants, while 40 min of heat treatment resulted in ~50% viable wild-type spores and less than 10% viable mutant spores (Fig. 5). The heat sensitivity of these mutants could be complemented by introducing a copy of a wild-type gene into the corresponding mutant strain (data not shown). An *rpfa swlB swlC* triple mutant was more sensitive to heat than any of the single mutants (Fig. 5). Taken together, these data suggest that

the activities of all four cell wall hydrolases are critical for the development of dormant, heat-resistant spores.

We also tested the single and multiple mutants for sensitivity to detergent, lysozyme, and cell wall antibiotics, as spore and cell wall defects have been associated with increased sensitivity to these chemical insults. None of the mutants were found to be more sensitive to these compounds than the wild-type strain.

Given that heat sensitivity is correlated with spore defects, SEM was used to compare the appearances of spores of wild-type and mutant strains (Fig. 6). We found that all four single hydrolase mutants exhibited abnormal spore morphologies. The *swlA* mutant spores failed to “round out” like wild-type spores and were variable in size, suggesting that there was a defect in the placement of sporulation septa. The *rpfa*, *swlB*, and *swlC* mutant spores were also heterogeneous in size and displayed a distinctive spore separation that yielded spores having an unusual cylindrical shape (Fig. 6). A similar cylindrical spore phenotype was observed for an *rpfa swlB swlC* triple-mutant strain (data not shown). Bright-field light microscopy and DAPI staining of the wild-type and mutant strains confirmed the abnormal shape and size of the mutant spores, revealing that despite the unusual spore separation and septum placement, DNA segregation was unaffected. To further probe the nature of the cylindrical spores observed for *rpfa*, *swlB*, and *swlC* mutants, TEM was conducted. We found that the spores were fully separated but that they were cylindrical when they were in spore chains (Fig. 7A) (they appeared to be rectangular in TEM cross sections); these chains were unlikely to represent an early stage of sporulation, as they were typically found together with abundant free spores, which are characteristic of mature sporulating cultures. The cylindrical spore conformation was not maintained following the liberation of individual spores, although some mutant spores appeared to be more oblong than round, which may be a reflection of the different spore sizes (Fig. 7A).

To further characterize the mutant spores, we conducted a quantitative examination of spore diameter and spore wall thickness using images obtained by TEM. We found no change

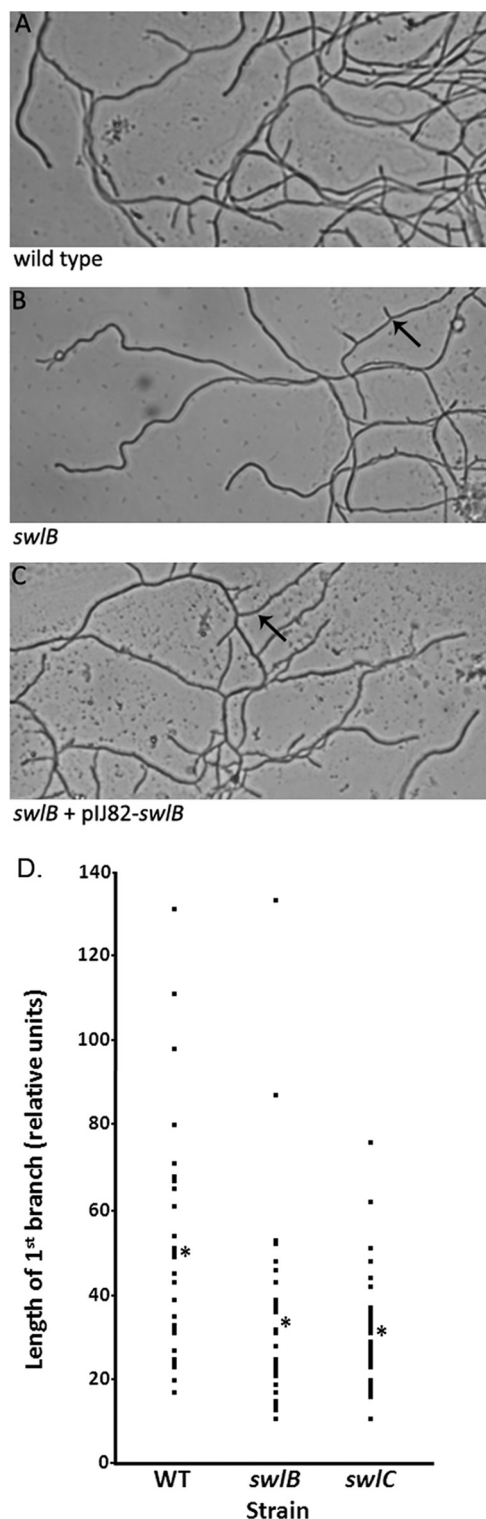


FIG. 4. Defects in vegetative growth for the *swlB* mutant: light microscope images of (A) wild-type strain, (B) *swlB* mutant, and (C) *swlB* mutant/pIJ82-*swlB* vegetative hyphae grown for 18 h on coverslips inserted into MS agar plates. While wild-type hyphae frequently extend significant branches, the arrow in panel B indicates the stunted branching observed for the *swlB* mutant. When a wild-type copy of *swlB* was introduced into the mutant on a plasmid, wild-type branching was restored, as indicated by the arrow in panel C. The *swlB* mutant also produced apparently longer hyphae than the wild-type

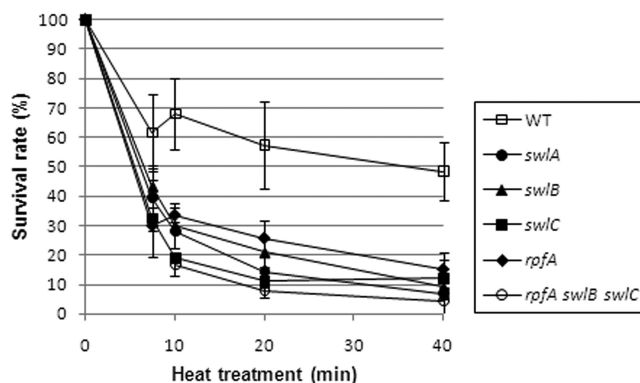


FIG. 5. Assay of the heat sensitivity of wild-type and cell wall hydrolase mutant spores. Spores were tested for the ability to survive heat shock at 60°C for the times indicated. Approximately 300 heat-shocked spores were spread on MS agar and incubated for 5 days, and their survival rates were calculated (see Materials and Methods). After a 40-min heat treatment, all mutant strains were at least threefold more heat sensitive than the wild-type strain, and the *swlA* mutant was the most heat sensitive of the single mutants, exhibiting a fivefold increase in heat sensitivity. Each value is the average of three replicates, and the standard error was calculated for the survival rate at each time point. WT, wild type.

in overall spore diameter for any of the mutants compared to the wild type (data not shown); however, all four individual hydrolase mutants possessed significantly thinner spore walls, which appeared to be on average only approximately one-third as thick as the wild-type spore walls (Fig. 7B and C).

***swlA* and *rpfB* mutants are delayed in spore germination.** As our investigations suggested that the four hydrolase gene products played a role in both vegetative growth and the formation of dormant spores, we were interested in determining whether these gene products also contributed to spore germination. Germination of both wild-type and mutant strains was assessed by incubating spores on MS agar and then scoring the frequency of germ tube emergence. No mutant strain was overwhelmingly defective in germination capability; however, the *swlA* and *rpfA* mutant strains reproducibly initiated germination more slowly than the wild type although by 11 h, spores of all strains were fully germinated (Fig. 8). The germination delay was, however, statistically significant only at 3 h for both mutant strains ( $P < 0.01$ ). All other mutant strains displayed germination kinetics similar to those of the wild-type strain. The germination defects of the *rpfA* and *swlA* mutants could be complemented by introducing a copy of the wild-type gene into the mutant strain (data not shown).

## DISCUSSION

The morphological development of *S. coelicolor* is tightly choreographed, and the different stages of development were expected to have unique requirements for cell wall remodeling.

strain. (D) Dot plot of first branch lengths for the wild-type, *swlB*, and *swlC* strains. Asterisks indicate the mean first branch length for each strain. The difference in branch length between each of the mutants and the wild type is statistically significant ( $P < 0.01$ ). WT, wild type.



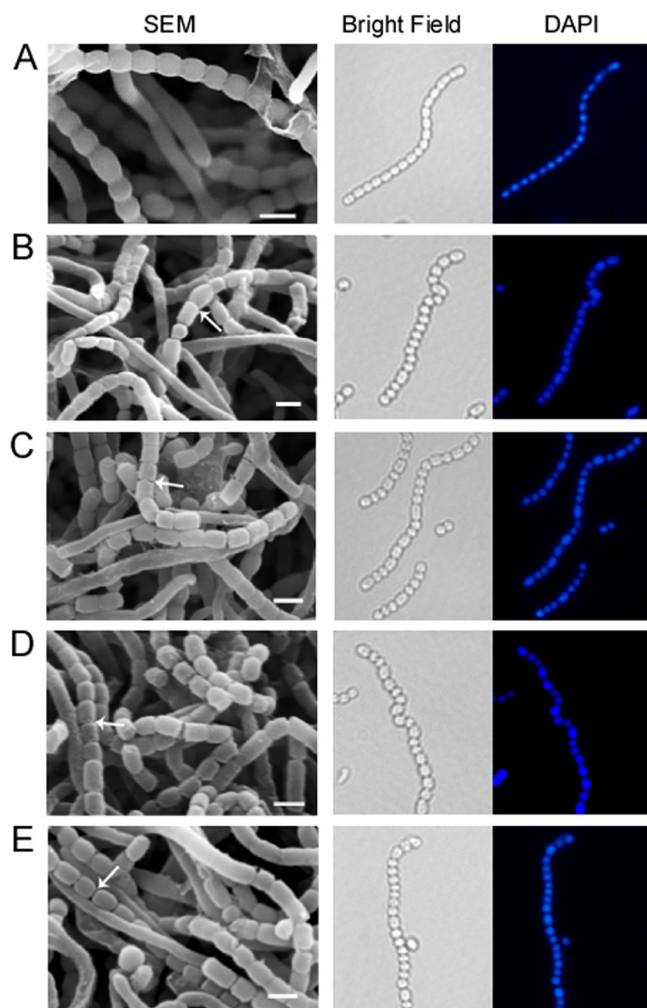


FIG. 6. Microscope images of (A) wild-type strain and (B) *swlA*, (C) *rpfA*, (D) *swlB*, and (E) *swlC* mutants. The panels on the left show SEM micrographs of wild-type and mutant spores after 5 days of growth on MS agar. While wild-type spores were rounded and a uniform size, the mutant spores were more “box shaped” and were irregular sizes. Bars = 1  $\mu$ m. The arrows indicate sites of enhanced spore separation. The panels on the right show bright-field images and fluorescence micrographs of wild-type and mutant strains after 4 days of growth on MS agar, followed by DAPI staining of coverslip impressions taken for each strain. Analysis of the mutant spore chains showed irregular spore sizes and shapes but no DNA segregation defects compared to the wild-type spore chains.

The complexity of the *S. coelicolor* life cycle is reflected by the number of cell wall hydrolases encoded in its genome; this number is significantly greater than the numbers encoded by other well-studied, but less morphologically complex bacteria, like *B. subtilis* and *E. coli* (24, 51). Given this, we expected that there may be very specific functions that could be ascribed to individual hydrolases acting at precise times during development or, alternatively, that significant redundancy would be observed for hydrolase function.

The hydrolases examined here were selected on the basis of shared upstream conservation, which was previously documented to have riboswitch-like characteristics by in silico analyses (4). Our results are consistent with this prediction, as we

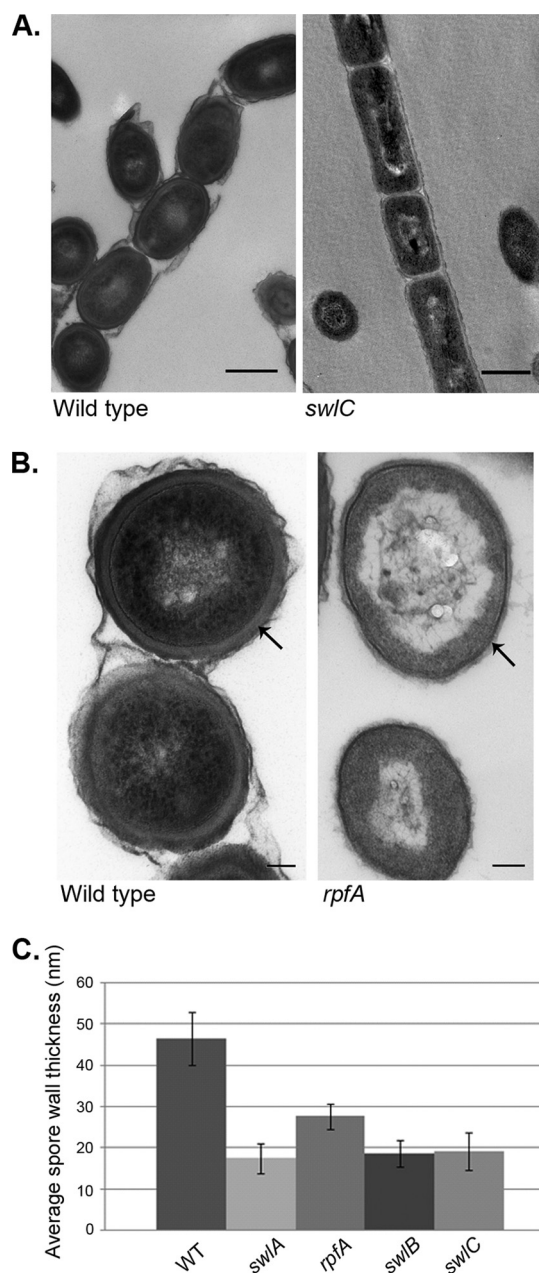


FIG. 7. TEM micrographs of wild-type and cell wall hydrolase mutant strains grown for 5 days on MS agar. (A) Cross sections of wild-type (left panel) and *swlC* mutant (right panel) spore chains, revealing cylindrical spores in the spore chains of the hydrolase mutant strain. Individual mutant spores, in contrast, are more rounded and are similar to wild-type spores (although they are longer in some cases). Bars = 500 nm. (B) Wild-type (left panel) and *rpfA* mutant (right panel) spores that are similar sizes but have different spore wall densities (arrows). Bars = 100 nm. (C) Quantitative comparison of spore wall thickness using the “Measure” function of ImageJ 1.41a. The bars indicate the means of at least 25 spore image measurements. The error bars indicate one standard deviation from the mean. WT, wild type.

found that each gene transcript had an extended, leader UTR that was >100 nt long. We reasoned that the associated gene products may have similar functions, as the downstream genes of conserved riboswitches in other systems invariably act in the

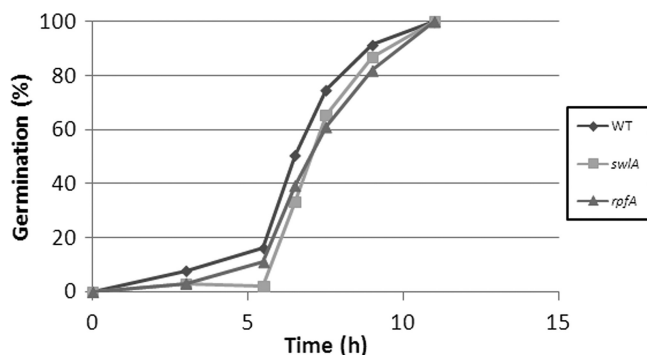


FIG. 8. Comparison of germination rates of the wild-type strain and *swlA* and *rpfA* mutants. Spores were spread on MS agar and were incubated at 30°C for the indicated periods of time. Germination was assessed using light microscopy. Germination experiments were conducted at least three times using independent spore stocks and involved quantifying the proportion of germinated spores in a population of >200 spores. The curves are representative germination curves and show that the proportion of germinated spores prior to 11 h was reproducibly less for the two mutant strains, although only the difference at 3 h was statistically significant ( $P < 0.01$ ). WT, wild type.

same metabolic pathway (41). We found that individual deletion of four hydrolase-encoding genes gave rise to strains with significant developmental defects, suggesting that the functions of the hydrolases were not (completely) redundant; whether the remaining 56 hydrolases encoded in the *S. coelicolor* genome have equally distinctive functions remains to be seen. The phenotypic effects of the hydrolase deletions were also not additive; a triple-mutant strain (*rpfA swlB swlC*) was slightly more heat sensitive than the corresponding single mutants, but it was morphologically indistinguishable from the single mutants during sporulation. This finding supported our proposal that the enzymes may all function in the same pathway or act together as part of a larger complex. Such complexes are not unprecedented in cell wall remodeling, as recent work with *M. tuberculosis* revealed that two Rpf proteins, RpfB and RpfE, bind to an NlpC/P60 endopeptidase termed RipA (23). We investigated the possibility of physical interaction between RpfA, SwlA, SwlB, and SwlC using a bacterial two-hybrid system (27), but our results did not support the hypothesis that there are interactions between these proteins (data not shown).

We also have evidence that suggests that several hydrolases in *S. coelicolor* are important during disparate developmental stages; our transcriptional analysis revealed that the majority of hydrolase genes examined were expressed most highly both early and late in development, and correspondingly, our phenotypic studies revealed vegetative and spore defects for at least two hydrolase mutants (*swlB* and *swlC* mutants). In comparison, in *B. subtilis*, there are dedicated hydrolases for spore germination, vegetative growth, and spore cortex maturation but no hydrolases that are directly involved in both vegetative growth and spore formation (51).

In addition to forming abnormal spores, the *swlB* and *swlC* mutant strains were also defective in extension of vegetative lateral branches. Recent work has shown that the DivIVA protein stimulates the formation and growth of lateral vegetative branches, presumably through the recruitment or activa-

tion of PG biosynthetic machinery at these sites (22). It will be interesting to determine whether the vegetative function of SwlB and SwlC can be correlated with that of DivIVA. The sporulation defects observed for the *swlB* and *swlC* mutants were also shared by the *rpfA* mutant. These strains had unusual spore chains, in which the spores appeared to be tethered together at the division sites, giving them a cylindrical appearance. This suggested that the enzymes encoded by these genes may be active during spore separation; however, this activity was not essential, as it was possible to liberate individual spores from the chains (Fig. 7). All hydrolase mutants, including the *swlA* mutant, which did not exhibit the spore tethering seen with the other mutants, were also heat sensitive and had much thinner spore coats than their isogenic parent strain, suggesting a further defect in spore coat assembly. Why cell wall hydrolase mutations result in thinner spore coats is not clear; however, this finding implies that spore wall biosynthesis is closely associated with peptidoglycan hydrolysis. Finally, we have shown that two cell wall hydrolases (encoded by *rpfA* and *swlA*) contribute to spore germination in *S. coelicolor* by facilitating the efficient outgrowth of germ tubes. Such a role for RpfA is consistent with the observed function of Rpf proteins in other actinomycetes (26, 37, 38). The RpfA and SwlA enzymes may act directly in degrading spore PG during germination or indirectly (for example, they may be involved in the formation of spore PG); in their absence, an altered substrate for germination-specific lytic enzymes may be generated, resulting in inefficient PG hydrolysis during germination. Germination defects have also been observed for *crp* mutants of *S. coelicolor*; however, these defects are thought to result, in part, from an abnormally thick spore wall, unlike the defect that we observed here (15, 43).

The spore defects observed for the hydrolase mutants (thin cell walls, heat sensitivity, and germination defects) were similar to the phenotypes of other developmental mutants. Heat hypersensitivity of spores has been noted previously for *whiD* and *mreB* mutants; additionally, *mreB* mutants are defective in germ tube elongation, and *whiD* mutant spores have thinner cell walls than wild-type spores (34, 35). Both *mreB* and *whiD* mutant spores are also irregular sizes, suggesting that there are defects in the positioning of spore septa similar to the defect seen for the hydrolase mutants examined here. *whiD* encodes a small protein that is a member of the “WhiB-like family” of proteins, whose function in sporulation has yet to be definitively determined (35). In contrast, MreB is proposed to polymerize to form an actin-like cytoskeletal scaffold for PG synthesis, and in *S. coelicolor* it is important primarily during aerial hypha formation and sporulation (34). In *B. subtilis*, the MreB isoform MreBH interacts with a PG-associated hydrolase (LytE), and this interaction is predicted to coordinate cell wall hydrolysis with cell wall synthesis (11); whether a similar interaction occurs in *S. coelicolor* remains to be determined. A final group of proteins that contribute to cell wall remodeling is the group that includes the recently characterized SsgA-like proteins (40). A model has been proposed in which these proteins control PG biosynthesis and hydrolysis during the sporulation process; however, the hydrolases examined here have not been implicated in this process (40).

PG is a major component of the gram-positive cell wall, and consequently, maintaining its integrity is of paramount impor-

tance. Cleavage of PG must therefore be a stringently controlled process, regulated both spatially and temporally to enable cell growth, division, and differentiation, while cell lysis is avoided. The conserved 5' UTR of the hydrolase genes examined here may represent a unique means of controlling hydrolase gene expression. The various transcription profiles for the different hydrolase genes suggest that this control is unlikely to be at the level of transcription; the conserved leader also does not contain any obvious transcriptional terminators (data not shown). Although riboswitch-mediated control has been proposed for this sequence, the possibility that this sequence is targeted for binding by a regulatory factor such as an RNA-binding protein or a small regulatory RNA cannot be excluded at this stage (45). It is worth noting, however, that this conserved sequence has been found upstream of genes in diverse bacteria, including *Mycobacterium*, *Bacillus*, and *Clostridium* strains (4), with many, but not all, of the associated genes encoding cell wall hydrolytic enzymes. Determining the function of the conserved sequence will therefore have broad implications and may reveal a novel control mechanism for cell wall hydrolase expression and activity.

#### ACKNOWLEDGMENTS

We thank Dave Capstick, Julia Swiercz, and Justin Nodwell for critical reading of the manuscript and helpful discussions, Dagmara Jakimowicz for microscopy advice, Dennis Claessen for helpful experimental suggestions, Eric Brown for his generosity in providing antibiotics, Marcia Reid for invaluable assistance with electron microscopy, and Nolan D'Souza, Lauren Brady, and Evelyn Miwa for assistance with experiments.

This work was funded by the Canada Research Chairs program, by a grant from the Natural Sciences and Engineering Research Council of Canada (NSERC discovery grant 312495), and by a seed grant from the Institute for Infectious Disease Research at McMaster University.

#### REFERENCES

- Altschul, S. F., W. Gish, W. Miller, E. W. Meyers, and D. J. Lipman. 1990. Basic local alignment search tool. *J. Mol. Biol.* **215**:403–410.
- Anantharaman, V., and L. Aravind. 2003. Evolutionary history, structural features and biochemical diversity of the NlpC/P60 superfamily of enzymes. *Genome Biol.* **4**:R11.
- Barreteau, H., A. Kovac, A. Boniface, M. Sova, S. Gobec, and D. Blanot. 2008. Cytoplasmic steps of peptidoglycan biosynthesis. *FEMS Microbiol. Rev.* **32**:168–207.
- Barrick, J. E., K. A. Corbino, W. C. Winkler, A. Nahvi, M. Mandal, J. Collins, M. Lee, A. Roth, N. Sudarsan, I. Jona, J. K. Wickiser, and R. R. Breaker. 2004. New RNA motifs suggest an expanded scope for riboswitches in bacterial genetic control. *Proc. Natl. Acad. Sci. USA* **101**:6421–6426.
- Bateman, A., E. Birney, R. Durbin, S. R. Eddy, K. L. Howe, and E. L. Sonnhammer. 2000. The Pfam protein families database. *Nucleic Acids Res.* **28**:263–266.
- Bendtsen, J. D., H. Nielsen, H. G. von, and S. Brunak. 2004. Improved prediction of signal peptides: SignalP 3.0. *J. Mol. Biol.* **340**:783–795.
- Bentley, S. D., K. F. Chater, A. M. Cerdeno-Tarraga, G. L. Challis, N. R. Thomson, K. D. James, D. E. Harris, M. A. Quail, H. Kieser, D. Harper, A. Bateman, S. Brown, G. Chandra, C. W. Chen, M. Collins, A. Cronin, A. Fraser, A. Goble, J. Hidalgo, T. Hornsby, S. Howarth, C. H. Huang, T. Kieser, L. Larke, L. Murphy, K. Oliver, S. O'Neill, E. Rabinowitch, M. A. Rajandream, K. Rutherford, S. Rutter, K. Seeger, D. Saunders, S. Sharp, R. Squares, S. Squares, K. Taylor, T. Warren, A. Wietzorrek, J. Woodward, B. G. Barrell, J. Parkhill, and D. A. Hopwood. 2002. Complete genome sequence of the model actinomycete *Streptomyces coelicolor* A3(2). *Nature* **417**:141–147.
- Bouhss, A., A. E. Trunkfield, T. D. Bugg, and D. Mengin-Lecreux. 2008. The biosynthesis of peptidoglycan lipid-linked intermediates. *FEMS Microbiol. Rev.* **32**:208–233.
- Bradford, M. M. 1976. A rapid and sensitive method for the quantitation of microgram quantities of protein utilizing the principle of protein-dye binding. *Anal. Biochem.* **72**:248–254.
- Buist, G., A. Steen, J. Kok, and O. P. Kuipers. 2008. LysM, a widely distributed protein motif for binding to (peptidoglycans. *Mol. Microbiol.* **68**:838–847.
- Carballido-López, R., A. Formstone, Y. Li, S. D. Ehrlich, P. Noirot, and J. Errington. 2006. Actin homolog MreBH governs cell morphogenesis by localization of the cell wall hydrolase LytE. *Dev. Cell* **11**:399–409.
- Cohen-Gonsaud, M., N. H. Keep, A. P. Davies, J. Ward, B. Henderson, and G. Labesse. 2004. Resuscitation-promoting factors possess a lysozyme-like domain. *Trends Biochem. Sci.* **29**:7–10.
- Cohen-Gonsaud, M., P. Barthe, C. Bagnieris, B. Henderson, J. Ward, C. Roumestand, and N. H. Keep. 2005. The structure of a resuscitation-promoting factor domain from *Mycobacterium tuberculosis* shows homology to lysozymes. *Nat. Struct. Mol. Biol.* **12**:270–273.
- Datsenko, K. A., and B. L. Wanner. 2000. One-step inactivation of chromosomal genes in *Escherichia coli* K-12 using PCR products. *Proc. Natl. Acad. Sci. USA* **97**:6640–6645.
- Derouaux, A., S. Halici, H. Nothaft, T. Neutelings, G. Moutzourelis, J. Dusart, F. Titgemeyer, and S. Rigali. 2004. Deletion of a cyclic AMP receptor protein homologue diminishes germination and affects morphological development of *Streptomyces coelicolor*. *J. Bacteriol.* **186**:1893–1897.
- Dramsli, S., S. Magnet, S. Davison, and M. Arthur. 2008. Covalent attachment of proteins to peptidoglycan. *FEMS Microbiol. Rev.* **32**:307–320.
- Elliot, M. A., N. Karoonuthaisiri, J. Huang, M. J. Bibb, S. N. Cohen, C. M. Kao, and M. J. Buttner. 2003. The chaplins: a family of hydrophobic cell-surface proteins involved in aerial mycelium formation in *Streptomyces coelicolor*. *Genes Dev.* **17**:1727–1740.
- Engel, H., B. Kazemier, and W. Keck. 1991. Murein-metabolizing enzymes from *Escherichia coli*: sequence analysis and controlled overexpression of the *slt* gene, which encodes the soluble lytic transglycosylase. *J. Bacteriol.* **173**:6773–6782.
- Firczuk, M., and M. Bochtler. 2007. Folds and activities of peptidoglycan amidases. *FEMS Microbiol. Rev.* **31**:676–691.
- Gust, B., G. L. Challis, K. Fowler, T. Kieser, and K. F. Chater. 2003. PCR-targeted *Streptomyces* gene replacement identifies a protein domain needed for biosynthesis of the sesquiterpene soil odor geosmin. *Proc. Natl. Acad. Sci. USA* **100**:1541–1546.
- Haiser, H. J., F. V. Karginov, G. J. Hannon, and M. A. Elliot. 2008. Developmentally regulated cleavage of tRNAs in the bacterium *Streptomyces coelicolor*. *Nucleic Acids Res.* **36**:732–741.
- Hempel, A. M., S. B. Wang, M. Letek, J. A. Gil, and K. Flärdh. 2008. Assemblies of DivIVA mark sites for hyphal branching and can establish new zones of cell wall growth in *Streptomyces coelicolor*. *J. Bacteriol.* **190**:7579–7583.
- Hett, E. C., M. C. Chao, A. J. Steyn, S. M. Fortune, L. L. Deng, and E. J. Rubin. 2007. A partner for the resuscitation-promoting factors of *Mycobacterium tuberculosis*. *Mol. Microbiol.* **66**:658–668.
- Holtje, J. V. 1998. Growth of the stress-bearing and shape-maintaining murein sacculus of *Escherichia coli*. *Microbiol. Mol. Biol. Rev.* **62**:181–203.
- Janssen, G. R., and M. J. Bibb. 1993. Derivatives of pUC18 that have BglII sites flanking a modified multiple cloning site and that retain the ability to identify recombinant clones by visual screening of *Escherichia coli* colonies. *Gene* **124**:133–134.
- Kana, B. D., B. G. Gordhan, K. J. Downing, N. Sung, G. Vostroktunova, E. E. Machowski, L. Tsenova, M. Young, A. Kaprelyants, G. Kaplan, and V. Mizrahi. 2008. The resuscitation-promoting factors of *Mycobacterium tuberculosis* are required for virulence and resuscitation from dormancy but are collectively dispensable for growth *in vitro*. *Mol. Microbiol.* **67**:672–684.
- Karimova, G., J. Pidoux, A. Ullmann, and D. Ladant. 1998. A bacterial two-hybrid system based on a reconstituted signal transduction pathway. *Proc. Natl. Acad. Sci. USA* **95**:5752–5756.
- Kieser, T., M. Bibb, M. Buttner, K. Chater, and D. Hopwood. 2000. Practical *Streptomyces* genetics. John Innes Foundation, Norwich, United Kingdom.
- Korat, B., H. Mottl, and W. Keck. 1991. Penicillin-binding protein 4 of *Escherichia coli*: molecular cloning of the *dacB* gene, controlled overexpression, and alterations in murein composition. *Mol. Microbiol.* **5**:675–684.
- Kuroda, A., and J. Sekiguchi. 1990. Cloning, sequencing and genetic mapping of a *Bacillus subtilis* cell wall hydrolase gene. *J. Gen. Microbiol.* **136**:2209–2216.
- LeClerc, D., and A. Asselin. 1989. Detection of bacterial cell wall hydrolases after denaturing polyacrylamide gel electrophoresis. *Can. J. Microbiol.* **35**:749–753.
- MacNeil, D. J., K. M. Gewain, C. L. Ruby, G. Dezeny, P. H. Gibbons, and T. MacNeil. 1992. Analysis of *Streptomyces avermitilis* genes required for avermectin biosynthesis utilizing a novel integration vector. *Gene* **111**:61–68.
- Margot, P., M. Wahlen, A. Gholamhosseinian, P. Pigot, and D. Karamata. 1998. The *lytE* gene of *Bacillus subtilis* 168 encodes a cell wall hydrolase. *J. Bacteriol.* **180**:749–752.
- Mazza, P., E. E. Noens, K. Schirner, N. Grantcharova, A. M. Mommaas, H. K. Koerten, G. Muth, K. Flärdh, G. P. van Wezel, and W. Wohlleben. 2006. MreB of *Streptomyces coelicolor* is not essential for vegetative growth but is required for the integrity of aerial hyphae and spores. *Mol. Microbiol.* **60**:838–852.
- Molle, V., W. J. Palframan, K. C. Findlay, and M. J. Buttner. 2000. WhiD and WhiB, homologous proteins required for different stages of sporulation in *Streptomyces coelicolor* A3(2). *J. Bacteriol.* **182**:1286–1295.



36. Mukamolova, G. V., O. A. Turapov, K. Kazarian, M. Telkov, A. S. Kaprelyants, D. B. Kell, and M. Young. 2002. The *rpf* gene of *Micrococcus luteus* encodes an essential secreted growth factor. *Mol. Microbiol.* **46**:611–621.
37. Mukamolova, G. V., A. S. Kaprelyants, D. I. Young, M. Young, and D. B. Kell. 1998. A bacterial cytokine. *Proc. Natl. Acad. Sci. USA* **95**:8916–8921.
38. Mukamolova, G. V., A. G. Murzin, E. G. Salina, G. R. Demina, D. B. Kell, A. S. Kaprelyants, and M. Young. 2006. Muralytic activity of *Micrococcus luteus* Rpf and its relationship to physiological activity in promoting bacterial growth and resuscitation. *Mol. Microbiol.* **59**:84–98.
39. Mukamolova, G. V., O. A. Turapov, D. I. Young, A. S. Kaprelyants, D. B. Kell, and M. Young. 2002. A family of autocrine growth factors in *Mycobacterium tuberculosis*. *Mol. Microbiol.* **46**:623–635.
40. Noens, E. E., V. Mersinias, B. A. Traag, C. P. Smith, H. K. Koerten, and G. P. van Wezel. 2005. SsgA-like proteins determine the fate of peptidoglycan during sporulation of *Streptomyces coelicolor*. *Mol. Microbiol.* **58**:929–944.
41. Nudler, E., and A. S. Mironov. 2004. The riboswitch control of bacterial metabolism. *Trends Biochem. Sci.* **29**:11–17.
42. Paget, M. S., L. Chamberlin, A. Atrih, S. J. Foster, and M. J. Buttner. 1999. Evidence that the extracytoplasmic function sigma factor  $\sigma^E$  is required for normal cell wall structure in *Streptomyces coelicolor* A3(2). *J. Bacteriol.* **181**:204–211.
43. Piette, A., A. Derouaux, P. Gerkens, E. E. E. Noens, G. Mazzucchelli, S. Vion, H. K. Koerten, F. Titgemeyer, E. De Pauw, P. Leprince, G. P. van Wezel, M. Galleni, and S. Rigali. 2005. From dormant to germinating spores of *Streptomyces coelicolor* A3(2): new perspectives from the *crp* null mutant. *J. Proteome Res.* **4**:1699–1708.
44. Ravagnani, A., C. L. Finan, and M. Young. 2005. A novel firmicute protein family related to the actinobacterial resuscitation-promoting factors by non-orthologous domain displacement. *BMC Genomics* **6**:39.
45. Romeo, T. 1998. Global regulation by the small RNA-binding protein CsrA and the non-coding RNA molecule CsrB. *Mol. Microbiol.* **29**:1321–1330.
46. Roth, A., W. C. Winkler, E. E. Regulski, B. W. K. Lee, J. Lim, I. Jona, J. E. Barrick, A. Ritwik, J. N. Kim, R. Welz, D. Iwata-Reuyl, and R. R. Breaker. 2007. A riboswitch selective for the queuosine precursor *preQ1* contains an unusually small aptamer domain. *Nat. Struct. Mol. Biol.* **14**:308–317.
47. Sambrook, J., and D. W. Russell. 2001. *Molecular cloning: a laboratory manual*, 3rd ed. Cold Spring Harbor Laboratory Press, Cold Spring Harbor, NY.
48. Sauvage, E., F. Kerff, M. Terrak, J. A. Ayala, and P. Charlier. 2008. The penicillin-binding proteins: structure and role in peptidoglycan biosynthesis. *FEMS Microbiol. Rev.* **32**:234–258.
49. Schleifer, K. H., and O. Kandler. 1972. Peptidoglycan types of bacterial cell walls and their taxonomic implications. *Microbiol. Mol. Biol. Rev.* **36**:407–477.
50. Setlow, P. 2003. Spore germination. *Curr. Opin. Microbiol.* **6**:550–556.
51. Smith, T. J., S. A. Blackman, and S. J. Foster. 2000. Autolysins of *Bacillus subtilis*: multiple enzymes with multiple functions. *Microbiology* **146**:249–262.
52. Steen, A., G. Buist, N. E. Kramer, R. Jalving, G. F. J. D. Benus, G. Venema, O. P. Kuipers, and J. Kok. 2008. Reduced lysis upon growth of *Lactococcus lactis* on galactose is a consequence of decreased binding of the autolysin AcmA. *Appl. Environ. Microbiol.* **74**:4671–4679.
53. Swiercz, J. P., Hindra, J. Bobek, H. J. Haier, B. C. Di Berardo, B. Tjaden, and M. A. Elliot. 2008. Small non-coding RNAs in *Streptomyces coelicolor*. *Nucleic Acids Res.* **36**:7240–7251.
54. Ursinus, A., and J. V. Holtje. 1994. Purification and properties of a membrane-bound lytic transglycosylase from *Escherichia coli*. *J. Bacteriol.* **176**:338–343.
55. Vollmer, W., B. Joris, P. Charlier, and S. Foster. 2008. Bacterial peptidoglycan (murein) hydrolases. *FEMS Microbiol. Rev.* **32**:259–286.
56. Winkler, W. C., A. Nahvi, A. Roth, J. A. Collins, and R. R. Breaker. 2004. Control of gene expression by a natural metabolite-responsive ribozyme. *Nature* **428**:281–286.